PAPER ID:0434
DOI: 10.18462/iir.compr.2021.0434

3D CFD MODELLING OF TWIN SCREW EXPANDERS USING REAL GAS EQUATION OF STATE AND REFPROP

Sham Rane, Ahmed Kovačević
City, University of London,
London, EC1V 0HB, UK, sham.rane@city.ac.uk

ABSTRACT

A twin screw expander's working chamber can be modelled in detail using 3D CFD and for a given operating condition the rotor configuration can be improved to achieve optimum internal expansion and maximize power recovery. In literature, it has been reported that use of an accurate fluid property definition such as NIST REFPROP database is essential to reproduce accurate pressure and temperature changes in the expansion chamber. However, when applied in the framework of a transient, 3D CFD computation, such databases have shown to increase the computational time by more than 50%. A numerically efficient alternative is to use a cubic equation of state. In this paper, some of the cubic equation of state definitions available in the ANSYS CFX flow solver for dry real gas properties have been evaluated in the application of an R245fa twin screw expander. The expander has a 4-5 lobe combination, 'N' rotor profile and a built-in volumetric expansion ratio of 4.5. Expander performance has been evaluated at 544 kPa filling pressure at 94.26°C using SCORG generated rotor grids for expander chamber, port grids for high pressure and low pressure ports. CFD results have been reported in terms of the internal pressure and temperature variation, mass flow rate, and indicated power output. Under the same operating condition, the CFD computational model is evaluated using NIST REFPROP database and the deviation in results are compared.

Keywords: Twin Screw Expander, CFD, SCORG, Real Gas Cubic Equation of State, R245fa, NIST-REFPROP

1. INTRODUCTION

Turbines and volumetric expanders working on organic Rankine cycles (ORCs) are being widely deployed for power generation at low and medium range of 3 to 50 kW. Typically these are used for waste heat recovery from industrial processes or as bottoming cycle of a primary Rankine cycle steam power plant. Smith et al. (2011) presented analysis of a twin screw wet steam cycle system to recover power from engine exhaust gases in the 300 - 450°C temperature range, with comparable efficiencies to turbine-driven systems. Admitting the steam to the twin screw expander as wet vapour was proposed to be a preferable option over turbines that cannot be used to expand vapours from this state. Some of the early studies such as Smith (1993) have shown that provided two-phase expanders can be made to attain adiabatic efficiencies of more than 75%, the Trilatral Flash Cycle system can produce outputs of up to 80% more than simple Rankine cycle systems in the recovery of power from hot liquid streams in the 100 - 200°C temperature range. For heat sources at lower temperatures of up to 200°C, organic fluids such as R134a (Tetrafluoroethane) or R245fa (1,1,1,3,3-Pentafluoropropane) or light hydrocarbons are commonly used due to lower latent heat, positive temperature-entropy slope of the saturation vapor line and other suitable properties of these fluids resulting in better cycle efficiencies. Smith et al (2011) highlighted another vital factor associated with steam that it has very low vapour pressure at condensing conditions required in Rankine cycles when rejecting heat to the ambient. Very low vapour pressure results into very high specific volume, thus requiring large and expensive turbine systems. On the other hand, organic fluids have considerably higher vapour pressure, higher density at condensing conditions and hence the expander size required is smaller resulting in high power density machines. The current research work is motivated from some of the results reported in recent literature on use of CFD models for performance evaluation of twin screw expanders used in ORC systems. Papeš et al. (2015) presented a CFD analysis of a 7 kW twin screw expander in an ORC system with R245fa working fluid using ANSYS FLUENT solver. They tested alternative specifications of properties of R245fa using the ideal

gas equation of state, the Aungier Redlich Kwong equation of state and the CoolProp library. It was reported that the difference in power output between the ideal gas equation of state and the ARK equation of state was 8% and between ARK equation of state and CoolProp database was negligible for the operating conditions taht were analysed. Along with this study, Abdelli (2015) in his thesis has reported analysis of the expansion process corresponding to the same twin screw expander but with a simplified geometry with square cross section. Dynamic mesh using layering algorithm in ANSYS FLUENT solver was used for the volumetric expansion and piston linear motion. In the ORC operating conditions (0.1-2 MPa and 300-450ºK), the ARK equation of state showed maximal pressure deviations of 15% comparing to CoolProp database. For specific heat, the deviations were a maximum of 10% for the ARK equation of state, while the ideal gas had a maximum of 30%. The accuracy of the NIST REFPROP (Lemmon et al. 2018) and the CoolProp databases were identical. The 3D CFD calculations of twin screw expander with 4-6 lobe, running at 6000rpm, were performed for an expansion process from 0.6-0.1 MPa and 400-350ºK. In these calculations with close to 2 million cell count, it was observed that the time required is twice when calculating with the CoolProp database as compared to ARK equation of state. It was not clear as to the level of solver convergence that was used for comparison or how the local variation of fluid properties differed, within the expander.

In this paper, some of the cubic equation of state definitions available in the ANSYS CFX flow solver for dry real gas properties have been applied in the modelling of 3 kW twin screw expander (Rane et al., 2020). The objective of this analysis was to evaluate computational accuracy in prediction of expander performance and the flow solver's computational time requirements when using the real gas equation of sate models in comparison to the specification of properties through NIST REFPROP fluid database. The expander has a 4-5 lobe combination, 'N' rotor profile and a built-in volumetric expansion ratio of 4.5. Expander performance has been evaluated at 544 kPa filling pressure at 94.26℃ and 175 kPa discharge pressure (Bianchi et al., 2019) using SCORG generated rotor grids for expander chamber, port grids for high pressure and low pressure ports. Observed differences in the CFD results have been reported in terms of the internal expansion pressure and temperature variation, mass flow rate, and indicated power output. Local variation of temperature and specific volume in the main and gate rotor chambers has been compared. Under the same operating condition, the CFD computational model is evaluated using NIST-REFPROP database and the deviation in results are compared.

2. TWIN SCREW EXPANDER CFD MODEL

CFD model of the twin screw expander is based on the use of numerical grids that deform with flow time in order to achieve positive volumetric displacement of the chambers. Kovačević and Rane (2013) have presented 3D CFD analysis of a dry air twin screw expander. In this study, the two rotors were each contained in a separate grid and were connected together thorugh non-conformal interfaces. Such interfaces simplify the grid generation procedure but are prone to mass imbalance and leakage over-estimation in the CFD solution. Recently a new grid generation technique has been introduced by the authors which contain both the main and gate rotors in a single grid domain and provide better accuracy to the results (Rane and Kovačević, 2017). These single domain rotor grids are generated by SCORG tool and have been used here for the CFD model as shown in Fig. 1. The expander operating condition of 544kPa filling at 94.26℃ and discharge pressure of 175kPa was selected at 3000 rpm rotor speed.

2.1. Rotor Grid Generation

Fig. 2 shows the details of the rotor grid in one of the cross section. The entire rotor grid is made of hexahedral cells and grid quality is optimized for smoothness, expansion factor and orthogonality, by using a partial diffierential equation based quality improvement procedure. Further details of the grid generation can be found in Rane and Kovačević (2017). In this case study, the rotor grid have 200 nodes circumferentially on the profile, 7 nodes radially and 136 axial sections. Table 1 summarises the CFD grid size in the rotor and the ports. In the rotor domain the node coordianates are updated by the flow solver with every time step, but the total count remains the same thus ensuring a conservative solution of the transport equations as described in Rane and Kovačević (2017). The ports are stationary and get connected to the deforming rotor domain through non-conformal interfaces. Important grid quality metrices are in Table 1 and there values are suitable for numerical stability and accuracy of most of the flow solvers in use.

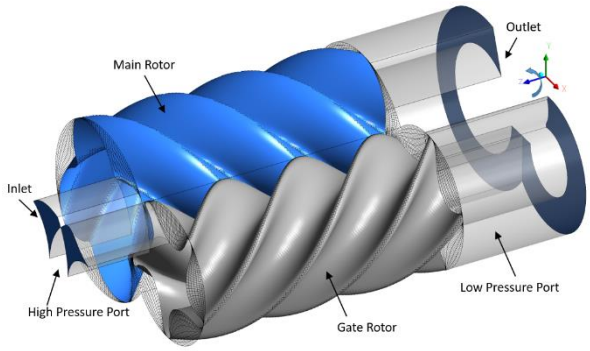

Figure 1: Expander CFD model

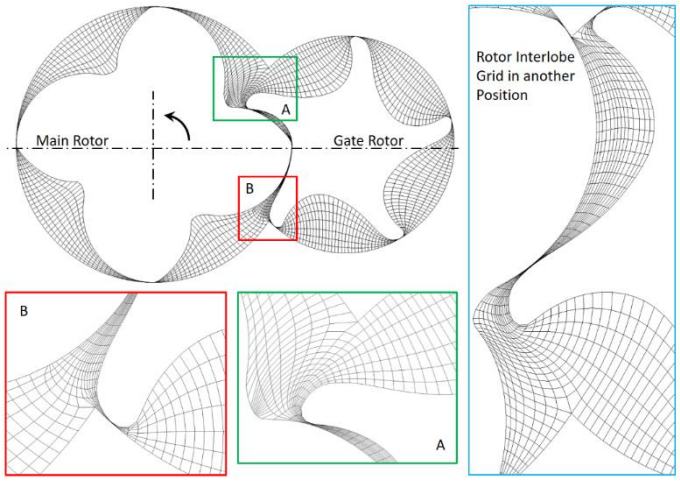

Figure 2: Details in the cross section of the rotor grid

Table1. CFD grid size and quality metrices

	Nodes	Cells	Orthogonal Angle		Expansion Factor		Aspect Ratio	
			Average	Minimum	Average	Maximum	Average	Maximum
Rotor	431550	380800	64.7	15.1	1.6	632.0	20.9	949.0
LP Port	81918	70400	76.9	34.6	1.1	2.0	2.0	4.0
HP Port	5292	4000	59.1	11.1	1.1	2.0	18.7	45.0

2.2. CFD solver settings

ANSYS CFX solver was used here for the calculations. Redlich and Kwong equation of state as defined in Eq. (1) has been used along with the Soave-RK and Aungier-RK variants.

$$p = \frac{R_s T}{v - b} - \frac{a}{\sqrt{T} v (v + b)} \qquad \text{Eq. (1)}$$

$$a = 0.42748 \frac{R_s^2 {T_c}^{5/2}}{p_c}, b = 0.08662 \frac{R_s T_c}{p_c}$$

The Peng Robinson equation of state model is an improvement over the SRK model. The definition is shown in Eq. (2) and is accurate at the critical point as well as the expander operating range.

$$p = \frac{R_s T}{v - b} - \frac{\alpha(T)\, a}{v^2 + 2bv - b^2} \qquad \text{Eq. (2)}$$

$$a = 0.45724 \frac{R_s^2 {T_c}^2}{p_c}, b = 0.0778 \frac{R_s T_c}{p_c}$$

$$\alpha(T) = \left(1 + n\left(1 - \sqrt{\frac{T}{T_c}}\right)\right)^2, n = 0.37464 + 1.54226\omega - 0.26992\omega^2$$

The advection scheme was set as first order upwind, time descritization was set as fully implicit second order backward Euler and turbulence model of SST k-Omega with first order descritization was used. The boundary conditions at high pressure inlet were total pressure and temperature, while at the low pressure outlet were static pressure. Main and gate rotor were set as rotating walls with angular speed of 3000 and 2400 rpm respectively. Since the rotor grid were generated with a 2.25 degree rotation per step, the solver time step size was set at 1.25e–4 sec to achieve 3000 rpm speed of the main rotor. Specific heat was specified through a 4th order polynomial whoes coefficient were obtained through REFPROP and critical state temperature and pressure were supplied to generate a lookup table in the temperature range of 250 and 400 K, while the pressure range was between 25 and 6000 kpa. The formulation for the specific heat at reference state (101.325 kPa, 25°C) is in Eq. (3). Fluid specific properties for R245fa were $\omega = 0.3776$, boiling temperature = 288.29 K, $p_c = 36.51\ bar, T_c = 427.16$ K, $v_c = 259.7466$ cm3 × mol− 1 and molar mass = 134.05 kg×kmol–1.

$$\frac{c_p^0}{R_S} = c_0 T^0 + c_1 T^1 + c_2 T^2 + c_3 T^3 + c_4 T^4 \qquad \text{Eq. (3)}$$

$$c_0 = 6.39, c_1 = -0.0012577, c_2 = 0.00019441, c_3 = -4.7081e-07, c_4 = 3.8563e-10,$$

Dynamic viscosity and thermal conductivity were specified using the option of kinetic theory model and crictical density as an input. Each case was solved for four revolutions of the main rotor such that pressure, temperature and mass flow rate through the boundaries showed a cyclic repetation. Cycle averaged data from last four cycles was used for expander performance evaluation.

3. RESULTS AND DISCUSSION

The expander CFD model was evaluated with five specifications of R245fa properties as listed in Table 2. Results showing the comparison between the fluid models are presented here in terms of the expander performance, internal pressure variation during expansion cycle, local distribution of pressure, temperature and specific volume. Also, some of the computational metrices have been reported in order to compare the CFD calculation effort.

3.1. Performance prediction

Table 2 summarises the expander performance as predicted by the CFD model when using different specifications for the working fluid R245fa. The first case is NIST REFPROP database and specific through pre-generated interpolation table that is used by the solver during calculations. The other four cases use real gas cubic equation of state as described in Section 2 and are directly available in the solver to select as the fluid model.

Table2. R245fa fluid specification in expander's CFD model and comparison of performance data

Case	R254fa fluid Data	Flow (kg s^{-1})	(%)	Power (kW)	(%)	Specific Power (kW kg^{-1} s)	e_P (kW kg^{-1} s)	(%)
1	NIST REFPROP	0.25939		3.114		12.006		
2	Redlich Kwong	0.25677	1.01	3.091	0.74	12.038	0.15	1.27
3	Soave Redlich Kwong	0.25870	0.26	3.100	0.47	11.982	0.06	0.54
4	Aungier Redlich Kwong	0.25890	0.19	3.099	0.48	11.971	0.06	0.52
5	Peng Robinson	0.26012	0.28	3.115	0.04	11.977	0.03	0.28
6	Ideal Gas	0.23904	7.84	2.968	4.69	12.417	1.22	10.17

NIST REFPROP solution has been used here as a reference. It can be observed from Table 2 that RK equation of state has the highest deviation in estimation of flow, power and specific power, although it is within 1.2%. Whereas, PR equation of state is in close agreement with NIST REFPROP with negligible deviation in the order of 0.1%. Both SRK and ARK equation of state produce flow, power and specific power with a deviation of less than 0.6% with respect to NIST REFPROP and can be considered as accurate enough to be used in the selected

operating condition of the expander.

3.2. Pressure distribution

Geometrical characteristics of the expander such as chamber volume variation, high pressure filling area and low pressure discharge area variation with the main rotor angle are presented in Fig. 3a. The expander filling pressure was 544 kPa and the discharge pressure was 175 kPa. Fig. 3b shows the pressure distribution during the filling, expansion and discharge processes.

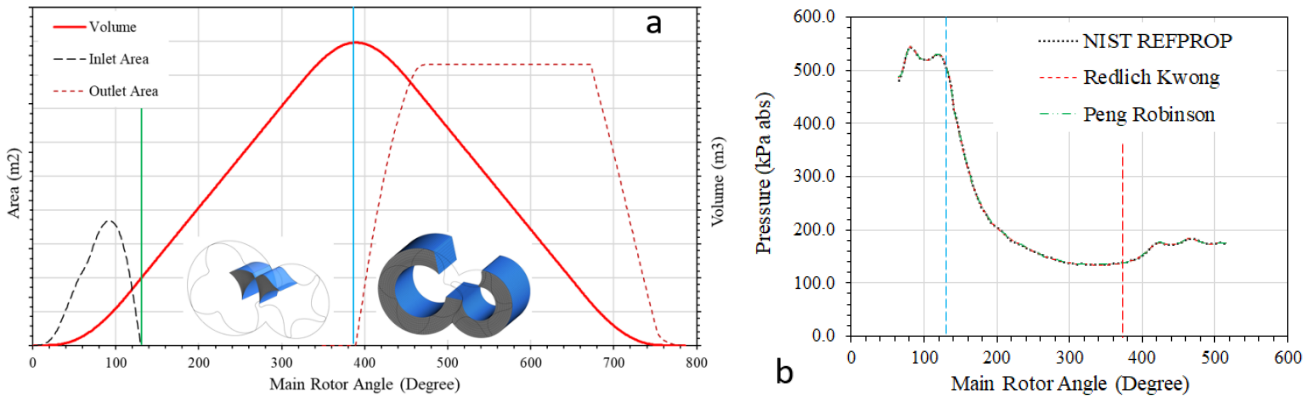

Figure 3: Geometrical characteristics of the expander and comparison of internal pressure during expansion

As observed from Fig. 3b, NIST REFPROP and both the equation of state models, RK and PR have identical pressure variation with main rotor angle. Pressure distribution using SRK and ARK, not plotted here for clarity, also overlapped with these results and indicate that in the operating conditions of the expander the real gas equation of state can be used with good accuracy. Fig. 4 shows distribution of instantenous pressure on the rotor surfaces and in the ports with NIST REFPROP fluid data. The pressure ranges from 100 to 544 kPa. Comparing these results with Fig. 3b, it is confirmed that the built-in volume index of 4.5 is creating over expansion in the screw chambers, before discharge to 175 kPa begins. Within each of the screw chambers, pressure distribution is uniform.

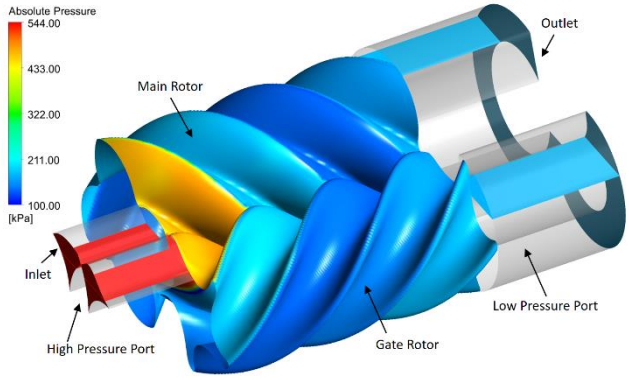

Figure 4: Instantenaous pressure ditribution

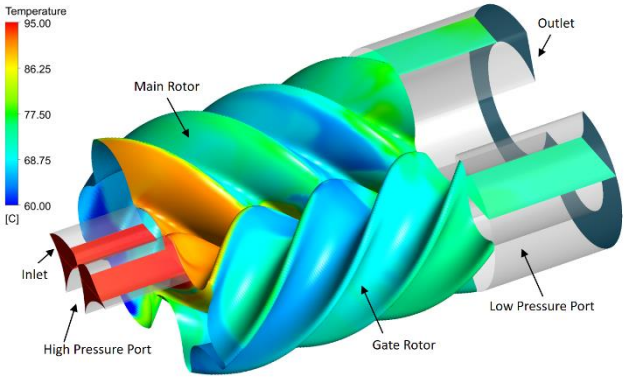

Figure 5: Instantenaous temperature ditribution

3.3. Temperature distribution

Fig. 5 shows distribution of instantenous temperature on the rotor surfaces and in the ports with NIST REFPROP fluid data. The temperature ranges from 60 to 95°C and within the screw chambers, a local variation is visible. This is due to the interaction of the gas volume in the chamber with leakage gas streams and the rotor dynamics.

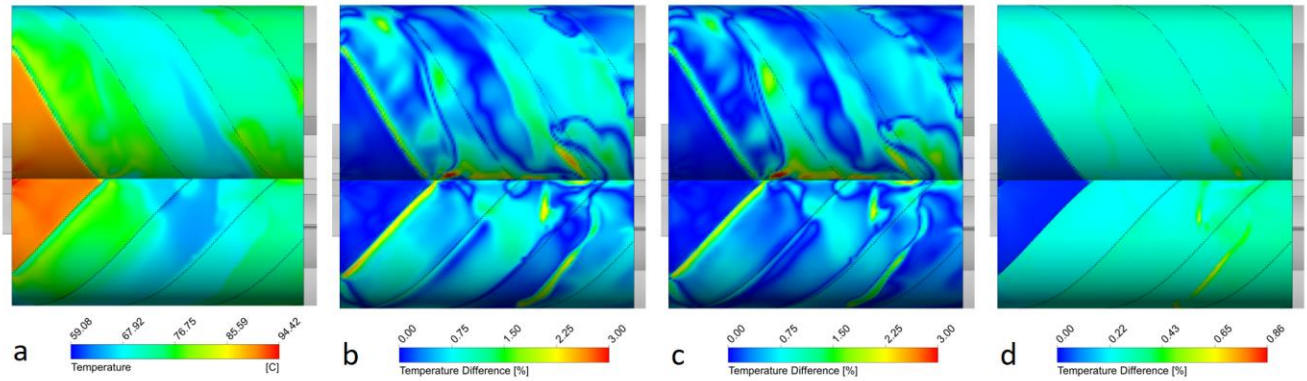

Figure 6: Comparison of local temperature distribution, a) REFPROP, b) Difference between RK and REFPROP, c) Difference between PR and REFPROP and d) Difference between RK and PR

Fig. 6a shows distribution of instantenous temperature on the rotor housing with NIST REFPROP fluid data. The distribution is in the same range as that on the rotor surfaces shown in Fig. 5. Fig. 6b and 6c shows the difference of instantenous temperature on the rotor housing with RK and PR equation of state respectively, compared with NIST REFPROP fluid data. Both RK and PR models have a maximum temperature deviation of less than 3%. With SRK and ARK models, the deviation was in the same order. Fig. 6d shows the difference of instantenous temperature between RK and PR equation of state models and maximum temperature deviation is less than 0.86%. All the four equation of state models considered here are thus accurate for the operating condition of the expander.

3.4. Specific Volume variation

Fig. 7a shows distribution of instantenous specific volume on the rotor housing surfaces with NIST REFPROP fluid data. Fig. 7b and 7c show the difference of instantenous specific volume on the rotor housing with RK and PR equation of state respectively, compared with NIST REFPROP fluid data. RK model has a maximum deviation of 17.53% in a few local cells present in the leakage gaps while it is slightly lower in case of PR model at 15.59% in similar local leakage regions. With SRK and ARK models, the specific volume deviation was in the same order. Fig. 6d shows the difference of instantenous specific volume between RK and PR equation of state models where the maximum deviation is 1.74%. On an average, the deviation in specific volume is less than 5% and all the four equation of state models considered here are accurate enough in the selected operating condition.

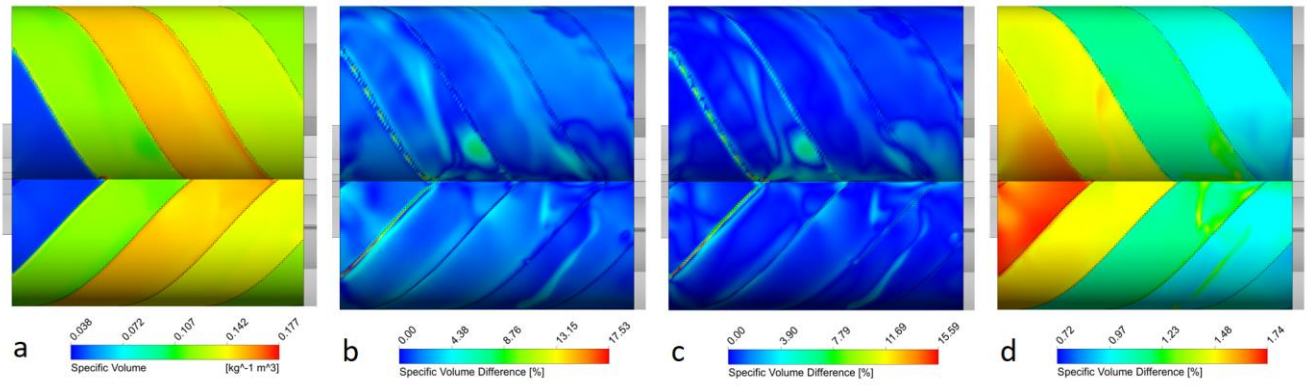

Figure 7: Comparison of local specific volume distribution, a) REFPROP, b) Difference between RK and REFPROP, c) Difference between PR and REFPROP and d) Difference between RK and PR

3.5. Computational metrices comparison

A summary of some of the computational metrices related to the CFD calculations are in Table 3. Case 1a is with NIST REFPROP fluid data. It has same number of solver iterations (equal to 5 per time step) as that of cases 2 – 5 which are with the real gas equation of state models. Case 1b is also with NIST REFPROP fluid data but here the number of solver iterations have been increased to 10 per time step. This was required to reach same level of numerical convergence as that obtained with the real gas cases 2 – 5. At the end of a time step, Case 1b residual levels were found to be 4.50E-05 for continuity, 4.70E-04 for energy and 4.50E-04 for momentum. These values have been used for normalization in Table 3 so that the difference in order of magnitude is apparent for Case 1a.

Table3. Comparison of computational metrices for the various fluid models

Case	R254fa fluid Data	Solver iterations	Normalized convergence level				CPU cores	CPU time
			Continuity	Energy	Momentum-w	average		(hr rev^{-1})
1a	NIST-REFPROP	5	1.53	2.16	1.64	1.78	6	3.95
1b	NIST-REFPROP	8	1.00	1.00	1.00	1.00	6	6.21
2	Redlich Kwong	5	0.81	1.16	1.13	1.03	6	3.88
3	Soave Redlich Kwong	5	0.81	1.14	1.13	1.02	6	3.79
4	Aungier Redlich Kwong	5	0.81	1.14	1.13	1.02	6	3.79
5	Peng Robinson	5	0.81	1.14	1.13	1.02	6	3.95
6	Ideal Gas	5	0.81	1.14	1.13	1.02	6	3.79

A mass imbalance was calculated between the cyclically averaged mass flow rate at the inlet and outlet of the expander. A high level of mass conservation (within 0.5%) was obtained with all the cases as shown in Table 3. The recorded CPU time in Table 3 indicates that Case 1b with higher number of solver iterations demanded by NIST REFPROP fluid database, required 57% higher calculation time to reach to the same order of numerical convergence as that of Cases 2 – 5 with real gas equation of state models.

4. CONCLUSIONS

A CFD model of twin screw expander has been analysed with R245fa gas as the working fluid. The objective of this analysis was to evaluate computational accuracy in prediction of expander performance, local variation of fluid properties and the flow solver's computational time requirements when using the real gas equation of sate models in comparison to the specification of properties through NIST REFPROP fluid database. The expander operating condition of 544kPa filling pressure at 94.26°C and discharge pressure of 175kPa was selected at 3000 rpm main rotor speed. Rotor and port grids were generated using SCORG grid generation tool and the flow solver ANSYS CFX was used for the CFD model. Following observations can be made from the analysis:

- In the operating range of the pressure and temperature, for R245fa gas, the Peng Robinson equation of state is the most accuarate in comparion to Redlich Kwong, Aungier Redlich Kwong and Soave Redlich Kwong models. Performance results of the expander were identical to the NIST REFPROP database specification in the CFD model. Local fluid properties such as temperature were deviating by less than 3% and maximum specific volume deviation was 15% in a few local cells present in the leakage gaps.

- Maximum deviation in local temperature was 0.86% and maximum deviation in local specific volume was 1.75% between the Redlich Kwong and the Peng Robinson equation of state models.

- Redlich Kwong has large deviation in the pressure and specific volume accuracy as compared to NIST REFPROP data close to the critical point. Hence, Redlich Kwong equation of state model cannot be used in this operating region. However, its variants Aungier Redlich Kwong and Soave Redlich Kwong as well as Peng Robinson models are suitable.

- When using NIST REFPROP database specification through property tables, the CFD solver required twice the number of sub-iterations per time step to reach the same level of numerical convergence and mass imbalance as that of the real gas models. This resulted into nearly 44% higher computational time requirement.

In future, it will be usefull to evaluate the real gas models at widely varying operating condition and with variety of working fluids. Similarly, various expander configurations such as number of lobes, volumetric expansion factor, rotor parameters, leakage clearances and operating conditions will provide further information.

NOMENCLATURE

p	pressure (Pa)	R	molar gas constant (8.314472 J×mol–1×K–1)
T	temperature (K)	v	specific volume (kg×m–3)
c_p	specific heat (J×kg–1×K–1)	R_s	specific gas constant (J×kg–1×K–1)
c	critical conditions	a, b	equation of state model parameters
ω	acentric factor	$a_0,\ b_0, c_0$	model constants
RK	Redlich Kwong	ARK	Aungier Redlich Kwong
SRK	Soave Redlich Kwong	PR	Peng Robinson

REFERENCES

Abdelli, L., 2015. CFD analysis of an expansion process using different real gas models. Masters dissertation, Department of Flow, Heat and Combustion Mechanics. Faculty of Engineering and Architecture. Ghent University, Belgium.

Bianchi, G., Rane, S., Fatigati, F., Cipollone, R., and Kovacevic, A. 2019. Numerical CFD Simulations and Indicated Pressure Measurements on a Sliding Vane Expander for Heat to Power Conversion Applications. Designs, 3, 31. doi : 10.3390/designs3030031

Kovačević, A., Rane, S. 2013. 3D CFD analysis of a twin screw expander. 8th International Conference on Compressors and their Systems. 417-429. Cambridge: Woodhead Publishing. ISBN 9781782421696.

Lemmon, E.W., Bell, I.H., Huber, M.L., McLinden, M.O. 2018. NIST Standard Reference Database 23: Reference Fluid Thermodynamic and Transport Properties-REFPROP, Version 10.0, National Institute of Standards and Technology, Standard Reference Data Program, Gaithersburg.

Papeš, I., Degroote, J., Vierendeels, J. 2015. New insights in twin screw expander performance for small scale ORC systems from 3D CFD analysis. Applied Thermal Engineering, 91, 535-546.

Rane S., Kovačević A., 2017. Algebraic generation of single domain computational grid for twin screw machines. Part I. Implementation. Advances in Engineering Software, 107, pp. 38-50. doi: 10.1016/j.advengsoft.2017.02.003

Rane S., Kovačević A., Stosic, N., Smith, I. K., 2020. Analysis of Real Gas Equation of State for CFD Modelling of Twin Screw Expanders with R245fa, R290, R1336mzz(Z) and R1233zd(E), doi: 10.1016/j.ijrefrig.2020.10.022

Smith, I. K. 1993. Development of the Trilateral Flash Cycle System: Part 1: Fundamental Considerations. Proceedings of the Institution of Mechanical Engineers, Part A: Journal of Power and Energy, 207(3), 179—194.

Smith, I. K., Stosic, N., Mujic, E., Kovacevic, A., 2011. Steam as the working fluid for power recovery from exhaust gases by means of screw expanders. Proceedings of the Institution of Mechanical Engineers, Part E: Journal of Process Mechanical Engineering, 225(2), pp. 117-125. doi: 10.1177/2041300910393429

Taleb, A., Sapin, P., Barfuß, C., Fabris, D., Markides, C., 2016. CFD analysis of thermally induced thermodynamic losses in the reciprocating compression and expansion of real gases. Journal of Physics: Conference Series, Volume 821, 1st International Seminar on Non-Ideal Compressible-Fluid Dynamics for Propulsion & Power, Italy.